to decay[24]; silver was then separated. For the determination of Ag^{115}, AgCl was precipitated from the initial target solution within ten minutes of bombardment. The precipitate was dissolved in the presence of cadmium carrier, the cadmium daughter activities were later purified and counted. Silver was separated as the chloride, iodide, sulfide, and the metal (using ascorbic acid in dilute NH_4OH solution). Iodide carrier was added during the Ag_2S precipitate and an $Fe(OH)_3$ scavenge was used. A scattering factor of 1.2 has been assumed for Ag^{112} and Ag^{113}. The 0.001-inch uranium targets used to determine Ag^{112} and Ag^{113} had no uranium guard foils, so a correction of 10 percent was added to the observed value for loss by recoils.[6] The Ag^{112} and Ag^{113} activities were resolved analytically[4] after subtraction of the Ag^{111} activity from the gross decay curve.

Cd^{115}, Cd^{115m}

The independent yields of these nuclides were determined by a rapid separation of AgCl from the target solution within ten minutes of bombardment. The Cd^{115} and Cd^{115m} activities were separated from the supernatant solution. Total mass 115 yields were also measured by determining the Cd^{115} and Cd^{115m} in day-old targets. Cadmium was separated as the sulfide from the uranium target solution after the uranium had been complexed with acetic acid and the pH adjusted to about 5. Scavenges of Sb_2S_3 from $2N$ HCl and $Fe(OH)_3$ from NH_4OH solution were performed and the cadmium precipitated as the sulfide from an NH_4OH solution. The CdS was dissolved in $1N$ HCl and placed on a Dowex A-1 column. The column was washed with $0.1N$ HCl and the cadmium eluted with $1.5M$ H_2SO_4. CdS precipitated from the H_2SO_4 solution was weighed and mounted for counting.

Cs^{136}

After the niobium had been precipitated with nitric acid, the supernatant solution was fumed with $HClO_4$ and the cesium perchlorate precipitated with ethyl acetate. Cesium silicotungstate was precipitated four times. The final sample was prepared as $CsClO_4$.

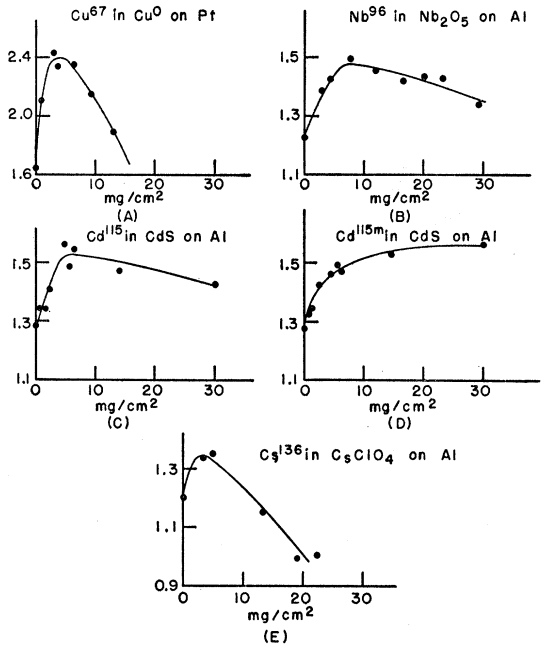

FIG. 8. Empirical corrections of counting data for the combined effects of self-scattering, self-absorption, and saturation back scattering.[24]

Sr^{89}, Zr^{97}, Pd^{109}, Pd^{112}, and Ba^{140}

These nuclides were determined in the same manner as in the previous paper.[10]

[24] H. G. Hicks and R. S. Gilbert, Phys. Rev. **94**, 371 (1954).

PHYSICAL REVIEW VOLUME 100 NUMBER 5 DECEMBER 1, 1955

Bremsstrahlung Spectrum from the Internal Target of a 22-Mev Betatron*

E. V. WEINSTOCK AND J. HALPERN
University of Pennsylvania, Philadelphia, Pennsylvania
(Received June 27, 1955)

The intensity and energy distribution of the bremsstrahlung photons produced in a betatron operating at 22 Mev have been determined by measurement of the energy spectrum of photoprotons ejected from deuterium. The protons were detected using a 0.15 cm thick NaI crystal followed by a 100-channel pulse-height analyzer. The photon beam was highly collimated in the forward direction. If one assumes the energy dependence of the cross section for the photodisintegration of deuterium as given by Hulthén, the computed bremsstrahlung energy distribution is in excellent agreement with the theoretical thin-target spectrum. The observed total intensity is that indicated by monitoring using an "R" thimble imbedded in 3.9 cm of Lucite.

INTRODUCTION

IN recent years a number of experiments[1–12] have been performed to determine the energy spectrum, and in some cases the absolute intensity, of the bremsstrahlung radiation produced in various targets by accelerator electrons in the relativistic energy range.

* Supported in part by the Air Research and Development Command and the joint program of the Office of Naval Research and the U. S. Atomic Energy Commission.

[1] P. K. S. Wang and M. Wiener, Phys. Rev. **76**, 1724 (1949).
[2] H. W. Koch and R. E. Carter, Phys. Rev. **77**, 165 (1950).
[3] R. H. Stokes, Phys. Rev. **84**, 991 (1951).
[4] Powell, Hartsough, and Hill, Phys. Rev. **81**, 213 (1951).
[5] J. W. DeWire and L. A. Beach, Phys. Rev. **83**, 476 (1951).
[6] V. E. Krohn and E. F. Shrader, Phys. Rev. **87**, 685 (1952).
[7] K. Phillips, Proc. Phys. Soc. (London) **A65**, 57 (1952).
[8] C. D. Curtis, Phys. Rev. **89**, 123 (1953).
[9] Motz, Miller, and Wyckoff, Phys. Rev. **89**, 968 (1953).
[10] P. C. Fisher, Phys. Rev. **92**, 420 (1953).
[11] K. Phillips, Proc. Phys. Soc. (London) **A67**, 669 (1954).
[12] R. M. Warner and E. F. Shrader, Rev. Sci. Instr. **25**, 663 (1954).

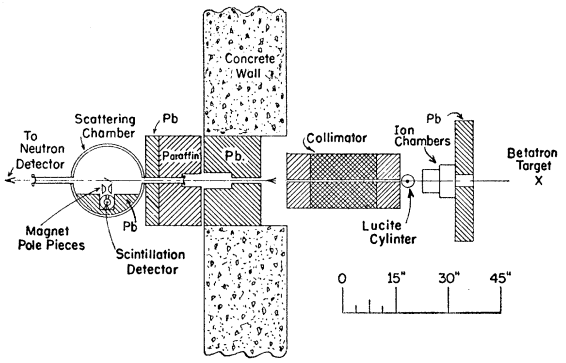

FIG. 1. General arrangement of apparatus.

The methods used have depended upon the detection of: the primary electrons after radiation[8,10]; the secondary electrons from processes such as pair production[2–5,12] and Compton scattering[9]; and the secondary protons from the photodisintegration of the deuteron.[1,6,7,11] The detectors used in the first three methods have been either magnetic spectrometers or magnetic cloud chambers, while the photoprotons from deuterium have in all such cases been detected in photographic emulsions. The results on the bremsstrahlung spectral shape have tended in general to verify the theory of Bethe and Heitler[13] as applied by Schiff[14] but with certain conflicts in the details. For instance, Krohn and Shrader[6] report a slight excess of photons in the high-energy end of the spectrum (for $E/E_m=0.8$, where E is the photon energy and E_m the initial energy of the radiating electron), while Koch and Carter[2] find an excess in the region $E/E_m=0.5$. In most cases, the spectral intensity has been normalized at an arbitrary energy.

Measurement of the bremsstrahlung radiation from the internal target of a betatron suffers somewhat from lack of control of the target geometry and to a certain extent from uncertainty as to its exact thickness. However, apart from its intrinsic interest, the spectrum must be known in order to measure photonuclear cross sections for reactions produced by such radiation. This paper is concerned with a determination of the spectral intensity and energy distribution of the radiation from the University of Pennsylvania betatron when operating at an energy of 22 Mev.

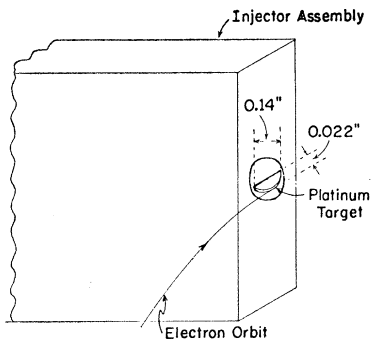

FIG. 2. Internal platinum target of betatron.

The method consists in the detection of 3000 photoprotons from a 14.8-mg/cm² deuterated paraffin sample and the measurement of their energies using a thin (0.15 cm) sodium iodide scintillation crystal and photomultiplier tube followed by a 100-channel pulse-height analyzer. The method has the advantage of speed in the gathering and analysis of data and depends essentially only on a knowledge of the deuterium photodisintegration cross section.

APPARATUS

Figure 1 shows the geometry and general experimental arrangement of the apparatus. The betatron is operated with a standard ceramic doughnut and injector assembly with associated internal target of the type supplied by the Allis-Chalmers Manufacturing Company. The material of the target is platinum in the shape of a segment of a disk (see Fig. 2) of base length 0.14 in. extending 0.022 in. from the injector assembly, and of thickness 0.015 in. near the tip. The electron orbit is tangent to the disk when undergoing expansion.

The x-ray beam from this target passes through the walls of the doughnut and through two aluminum ionization chambers whose current monitors the beam intensity (and when integrated the total amount of radiation), and is then collimated as described below before entering the detector chamber, which is located behind a 16-in. lead shield imbedded in the 2-ft concrete wall surrounding the betatron. Table I is a list of the compositions and thicknesses of absorbing materials in the beam between the doughnut target and the entrance to the detection assembly. A Victoreen 250-R thimble imbedded in the 3.9-cm-thick Lucite cylindrical block is used to calibrate one of the ionization chambers in terms of roentgens, and is removed from the beam during measurements of the x-ray spectrum.

The beam collimator, consisting of three parts, is shown in detail in Fig. 3. The collimation is achieved by a tapered hole through 8 in. of lead, the entrance and exit diameters being 0.136 in. and 0.161 in. respectively. The second section of the collimator consists of a region 15 in. long with a magnetic field of 3000 gauss produced by magnetized Alnico blocks in steel return rings, with a gap of 0.4 in. so that the magnets are out of the x-ray beam. Electrons in the beam are deflected in this region into aluminum inserts. Supplementary shielding is supplied by another section of 8 in. thick lead with a 0.5-in. opening, which does no further collimation. The total angular width of the beam after collimation is 0.00322 radian, producing a circular beam at the center of the detection chamber of 8-mm diameter.

[13] W. Heitler, *Quantum Theory of Radiation* (Oxford University Press, London, 1944), second edition, p. 164.
[14] L. I. Schiff, Phys. Rev. 83, 252 (1951).

The deuterated paraffin radiator and scintillation crystal assembly, located some ten feet from the betatron target and 4 feet from the exit of the collimator are contained in an evacuated brass cylinder 20 in. in diameter with entrance and exit snouts sealed by 10-mil aluminum windows for passage of the beam. The deuterated paraffin foil, 14.8 mg/cm² thick corresponding to a proton energy loss of 0.2 Mev for protons of 10 Mev energy, was prepared by pressing powdered deuterated wax at an elevated temperature between films of mylar in a press at 20 000 lb/in². It was then mounted on a frame with two other foils, one of ordinary paraffin of equivalent thickness and the other of platinum on which was plated a thin polonium alpha source. The frame, which placed the plane of the foils at an angle of 30 degrees with respect to the beam direction, was attached to a keyed shaft which entered the chamber through an *O*-ring seal in the floor. By sliding the shaft vertically, any one of the foils could be positioned in the beam, and when desired the entire assembly could be retracted into a well in the chamber bottom.

TABLE I. Absorbing materials in the x-ray beam.

Object	Composition	Atomic number	Thickness (gm/cm²)
Doughnut wall	O	8	1.21
	Al	13	0.352
	Si	14	0.708
	K	19	0.253
Ionization chambers	Al	13	4.67

The photoproton detector consisted of a square NaI(Tl) crystal measuring 0.780 in.×0.780 in.×0.065 in. mounted vertically on the face of a Dumont 6292 photomultiplier tube whose envelope was inserted vertically through a 2-in. O-ring seal in the chamber floor, leaving the tube base outside the vacuum system. The crystal was 6 in. from the radiators at an angle of 90° with respect to the beam direction. Over the crystal and photocathode was placed a polished aluminum dome with a window cut out for the passage of the particles to be detected. A cylindrical shield of $\frac{9}{16}$-in. iron lined on the inside with 0.060-in. mu-metal enclosed the part of the multiplier tube inside the vacuum chamber.

Although the NaI crystal was sufficiently thin so that an electron would lose only 1 Mev of energy traversing it, the number of secondary electrons from the radiator was large and straggling in the crystal gave energy losses up to 4 Mev. Consequently, a permanent magnet, whose field (4000 gauss) was horizontal and at right angles to the line from radiator to detector, was installed between magnet and radiator along with a 0.25-in. lead shield with rectangular hole. This arrangement prevented most of the secondary electrons and positrons from reaching the NaI.

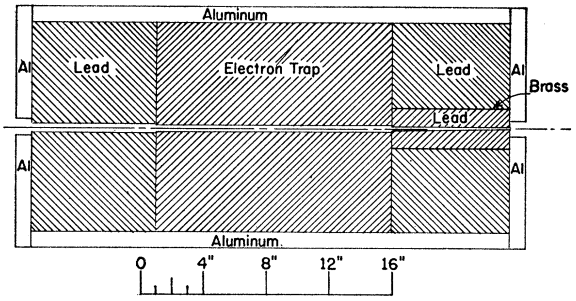

FIG. 3. Beam collimator.

The details of the crystal preparation and mounting (Fig. 4) are of some interest, especially because of the problem of evaporation of the NaI surfaces in vacuum. Although the rate of evaporation is not large, the evaporation process does cause the optical properties of the surfaces to vary with time. Therefore the back surface of the crystal was protected by cementing to it a square of Lucite $\frac{1}{16}$ in. thick, the cement being an epoxy resin called Bonding Agent R-313.[15] The front surface was covered by a nylon film thin enough to show interference colors. The nylon was the only material in the path of the photoprotons and its effect on their energies was negligible. One edge of the crystal-Lucite sandwich was cemented to a strip of aluminum foil, which in turn was cemented to the photomultiplier face. The aluminum foil prevents any light from reaching the photocathode directly through the interface between glass and crystal and tends to equalize all portions of the crystal as evidenced by increased resolution. Crystals prepared in this manner have been found to be stable over periods of months with a resolution of from 6 to 8% for the 5.3-Mev alpha particles of polonium.

After emerging from the detection chamber, the x-ray beam strikes a 7.5-g/cm² magnesium sample contained in a neutron detection assembly,[16] and the rapid change in the magnesium neutron yield with energy of the betatron serves to monitor the energy of the betatron.

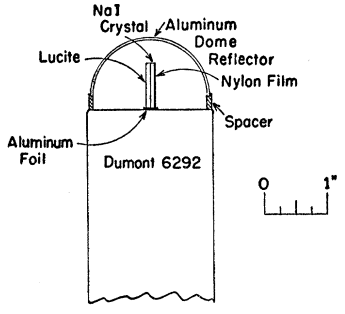

FIG 4. NaI scintillator and mounting. The proton entrance window is not shown.

[15] Carl H. Biggs Company, Los Angeles, California.
[16] Halpern, Mann, and Nathans, Rev. Sci. Instr. 23, 678 (1952).

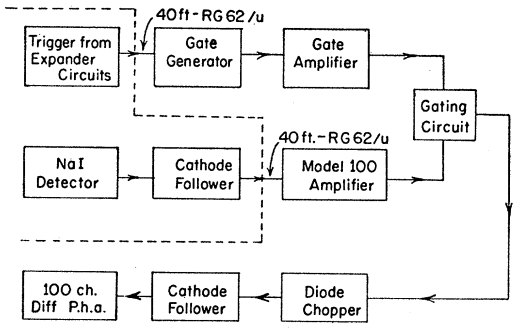

FIG. 5. Block diagram of circuitry.

The output pulses from the photomultiplier, operated at 1370 volts, enter a cathode follower the output of which feeds through 40 feet of cable a Los Alamos Model 100 amplifier in the control room of the betatron (Fig. 5). The amplified pulses are then fed into a gating circuit, which passes only those pulses which occur during a 100-microsecond period bracketing the x-ray pulses from the betatron and rejects any delayed background arising from induced radioactivity of the materials surrounding the detector, and from other sources. The output then enters a chopping circuit which subtracts ten volts from the amplitudes of the pulses to prevent the small but numerous electron pulses from reaching the 100-channel differential pulse-height analyzer with its relatively long dead time of 60 milliseconds. The differential analyzer, of the Wilkinson type[17] with a measured linearity of 0.1 volt, is followed by a ball-drop mechanism to record and display the data. Ball bearings are dropped into 100 channels milled into a Lucite block at a maximum handling rate of 12 equally spaced events per second per channel, a rate entirely adequate for this experiment where the overall counting rate for all channels never exceeded 6 counts per minute.

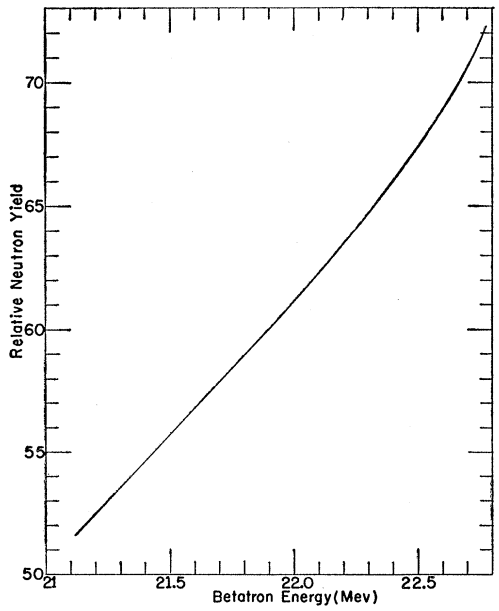

FIG. 6. Energy response of $Mg(\gamma,n)$ beam monitor.

[17] D. H. Wilkinson, Proc. Cambridge Phil. Soc. 46, 508 (1950); Los Alamos Scientific Laboratory Report LA-1565, 1953 (unpublished).

PROCEDURE

The experiment consists of a determination of the pulse height distribution of photoprotons from the deuterated paraffin radiator, with background removed by measuring the equivalent distribution from a normal paraffin radiator under identical bombardment conditions. Since the data are taken over a two-week interval of time, suitable precautions are necessary to insure energy stability of the betatron and gain and resolution stability of the detector. Furthermore, absence of pile-up effects must be insured.

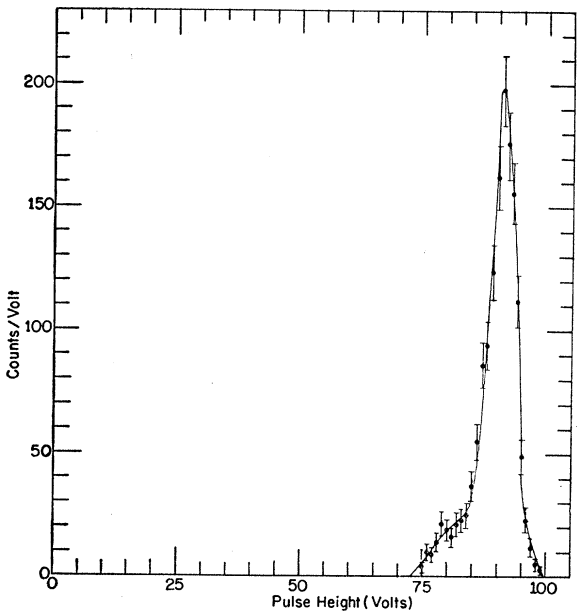

FIG. 7. Detector resolution curve for alpha particles of polonium.

Although the measurement of background using normal paraffin in the beam eliminates protons arising from the (γ,p) reaction in the carbon of the radiators, this is no serious problem because of the high $C(\gamma,p)$ threshold. There can be no protons from this cause in excess of 4 Mev, and the yield is low at this energy as seen by the background counting rates. Neutrons from the deuterium can give recoil counts in the Na and I of the detector with maximum energy of only 1.6 Mev.

The betatron was operated at an energy of 22.0 ± 0.1 Mev, expansion of the electron orbit taking place at the peak of the magnet cycle. The machine's energy was determined by reference to the (γ,n) threshold of a bismuth sample replacing magnesium in the neutron detection house used to monitor the betatron energy,

and is good to ±0.1 Mev. The energy stability of the machine was monitored continuously throughout the experiment by the yield of neutrons from the magnesium sample (whose neutron yield sensitivity to betatron energy in the vicinity of 22 Mev is shown in Fig. 6). Again the energy was found to be stable to ±0.1 Mev.

At the start and end of each day's run the polonium alpha source was exposed to the detector and the pulse-height distribution measured to check both gain and resolution of the detector and the over-all performance of the electronic circuitry. Figure 7 shows a typical resolution curve so taken. The resolution was 8% and did not vary detectably throughout the runs. The position of the peak as determined in this manner was stable to ±2%.

As in previous photoproton work[18] the betatron expander pulse was adjusted to give an x-ray pulse of 60-microsecond duration as measured and monitored by an auxiliary scintillation counter off the beam axis near the collimator entrance. The absence of any pile-up effects under these operating conditions was checked by making runs at several different beam intensities with no observed changes in results. For the duration of the experiment the beam intensity was kept at approximately 30 roentgens per minute at 3 feet from the betatron internal target.

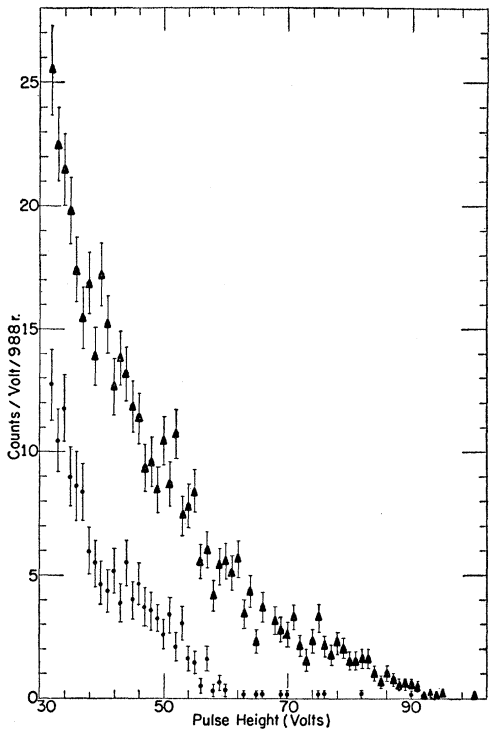

FIG. 8. Channel by channel plot of data. Photoprotons from deuterated paraffin and normal paraffin are shown. The circles are from normal paraffin.

RESULTS

Figure 8, representing the uncorrected data of the experiment, shows the actual number of counts per channel per 988 roentgens at the sample for both of the deuterated and normal paraffin radiators. A total of 3000 useful events was recorded for a total exposure of 10^4 roentgens. Subtraction of the background and grouping of the counts in 5-volt intervals leads to the curve of Fig. 9. Since the choice of end point is fairly critical in determining the energy scale the tail of the curve of Fig. 9 was drawn using the channel by channel plot as a guide.

Before conversion of this curve to the betatron bremsstrahlung energy distribution by the introduction of the $D(\gamma,p)$ cross section, corrections are necessary for the resolution of the detector and for the proton energy loss in the radiator. The unfolding of the effects of the detector resolution was done by successive application of the resolution function of Fig. 7 to a trial curve to give exactly the observed results. Actually, the only significant difference between the final derived curve and that observed occurs at the very end of the spectrum.

Having now fixed the end point of the spectrum of protons, the energy scale is determined from the kinematics of the photodisintegration of the deuteron. That is, an energy is ascribed to the end point corresponding to the energy of a proton produced at 90 degrees by a 22-Mev photon.[19] The scale in pulse height is now converted to proton energy in Mev.

The effect of finite thickness of deuterated paraffin radiator was removed by using the range-energy table

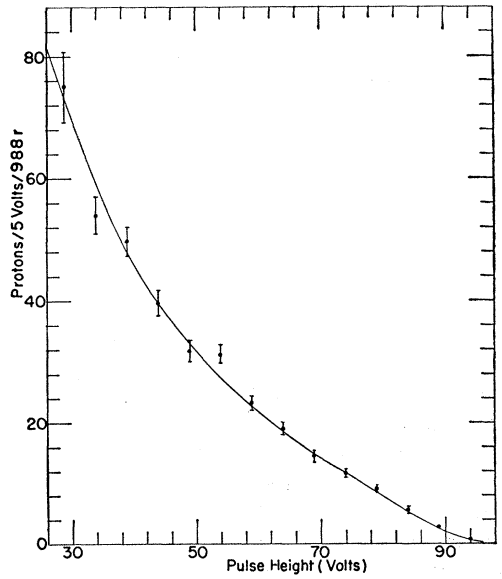

FIG. 9. $D(\gamma,p)$ yield in 5-volt intervals with background subtracted.

[18] E. V. Weinstock and J. Halpern, Phys. Rev. 94, 1651 (1954).

[19] J. Halpern and E. V. Weinstock, Phys. Rev. 91, 934 (1953).

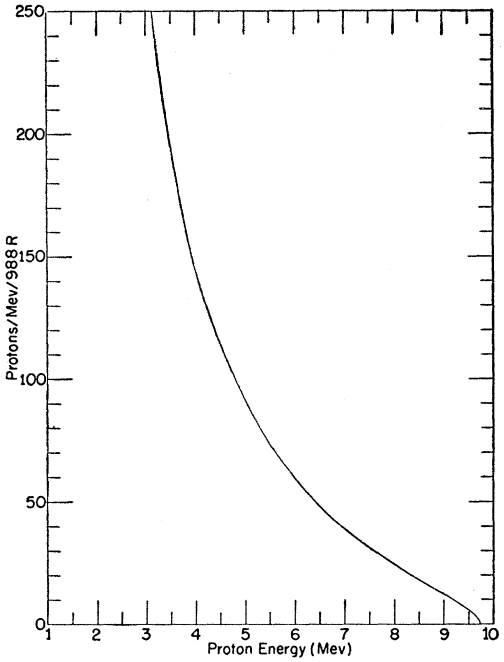

FIG. 10. Photoproton energy distribution from deuterium target corrected for detector resolution and target absorption.

of Rich and Madey[20] and a numerical calculation identical to that employed for unfolding the effects of detector resolution. Figure 10 shows the final proton energy distribution corrected for both resolution and absorption.

The observed bremsstrahlung spectrum is now computed by converting intervals of proton energy to intervals of photon energy and by application of the deuteron photodisintegration cross sections as given by the theoretical results of Hulthén and Nagel[21] (interpolated for a meson mass of 275 electron masses) which appear to give reasonable fit to existing data in the energy region of interest. Center-of-mass corrections for the proton energies at 90° are taken into account.[19] Knowledge of the number of deuterium atoms in the beam and the exact solid angle of the detector permit the bremsstrahlung distribution (solid curve) of Fig. 11 to be given in terms of number of photons per cm² per "R" per Mev. The angular distribution of the deuteron photodisintegration is assumed to have a $\sin^2\theta$ shape, although the introduction of a small symmetric component does not significantly alter the curve.

The dotted curve of Fig. 11 represents the bremsstrahlung spectrum computed from the Bethe-Heitler theory as applied by Schiff[14] modified for the absorption of the doughnut wall and ionization chambers. The absolute values of the ordinates of this curve depend on the conversion of photon intensity in ergs/cm² to R readings as measured by the Victoreen R thimble im-

[20] M. Rich and R. Madey, U. S. Atomic Energy Commission Report UCRL-2301, 1954 (unpublished).
[21] L. Hulthén and B. C. H. Nagel, Phys. Rev. **90**, 62 (1953).

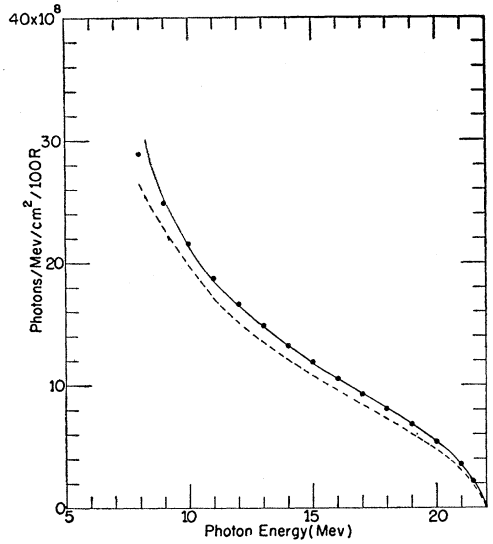

FIG. 11. Bremsstrahlung distribution. The solid curve is from the measurements while the dotted curve is the computed one. The circles are taken from the computed curve multiplied by the factor 1.09.

bedded in the Lucite.[22] Comparison of the measured and computed distributions is illustrated by the circles of the figure, which represent the computed values multiplied by a factor of 1.09.

DISCUSSION

The measured shape of the bremsstrahlung from the betatron as observed in the forward direction is in remarkable agreement with the Schiff thin-target computations with a discrepancy in absolute intensity of 9%. Possible sources of error in the intensity determination are of two types, namely, those involving the measurement of the solid angle of the detector, the thickness of the deuterated paraffin radiator, and the diameter of the collimated x-ray beam; and those involving the knowledge of the deuterium cross section and the conversion of ergs/cm² to R readings.

The total uncertainty due to the possible errors in the measurements of the apparatus geometry are estimated at not greater than about 5%. With similar errors possible in the knowledge of the deuteron photodisintegration cross section, the discrepancy in absolute intensity of the bremsstrahlung seems within the accuracy of the measurement, and the monitoring of the x-ray beam by the R thimble in 3.9 cm of Lucite thus provides a reliable measure of the beam intensity.

The data on spectral shape cannot be extended below a photon energy of 8 Mev because of increased background and consequently greater statistical uncertainty, and also because of the photoproton energy loss in the deuterated paraffin becomes excessive. In fact, the total thickness of the deuterated paraffin radiator corresponds to the range of a 3-Mev proton.

[22] Johns, Katz, Douglas, and Haslam, Phys. Rev. **80**, 1062 (1950).